

ANTONIUS¹✉

Ay Lie HAN²

MUSLIKH³

Nurti Kusuma ANGGRAINI⁴

¹ Universitas Islam Sultan Agung, Faculty of Engineering, Semarang, Indonesia

² Diponegoro University, Faculty of Engineering, Semarang, Indonesia

³ Universitas Muhammadiyah Yogyakarta, Faculty of Engineering, Yogyakarta, Indonesia

⁴ Semarang State University, Faculty of Engineering, Semarang, Indonesia

Investigation on strength and ductility of confined geopolymer concrete subjected to axial loads

Keywords: geopolymer, strength, ductility, confinement, analytical expression

Introduction

Background

Geopolymer concrete is a relatively new material, which has been extensively researched in the last two decades. The research carried out aims to develop concrete and more environmentally friendly materials. This is based on the fact that every production of 1 t of ordinary portland cement (OPC) will emit 1 t of CO₂ gas into the atmosphere (Bouzoubaâ et al., 1999). As a result, a greenhouse effect arises in the atmosphere and the temperature on the Earth's surface increases, it gets hotter, thus leading to an environmental problem. Therefore, reducing the use of portland cement must be a priority in the world of construction, also among practitioners. One way to do this is to develop and manufacture geopolymer concrete that

does not use 100% portland cement (Ekaputri & Triwulan, 2011; Owaied et al., 2021). Fly ash, which is obtained from burning coal and is pozzolanic and also cementitious according to ACI ACI 232 2R-96 standard (American Concrete Institution [ACI], 2002), is used to replace portland cement.

The mechanical characteristics of geopolymer concrete are not considerably different from the characteristics of concrete that uses OPC (OPC concrete), such as: compressive strength, tensile strength, modulus of elasticity, modulus of rupture, and other mechanical quantities (Hardjito et al., 2004; Diaz-Loya et al., 2011). The treatment effect in the process of making geopolymer concrete has a significant influence on increasing compressive strength and tensile strength (Triwulan et al., 2017). The mechanical properties of geopolymer concrete are also not significantly different from the mechanical properties of OPC concrete, even though the alkaline activator used is low, namely 4% (Romadhon et al., 2022). This material is also identified to have good resistance to chloride penetration and abrasion (Nagajothi et al., 2022; Wong, 2022).

In stress–strain behavior, geopolymer concrete also has a similar curve shape to normal concrete, especially in the behavior before peaking. However, geopolymer concrete has a different post-peak behavior from the post-peak behavior of normal concrete. In the post-peak curve behavior, the geopolymer concrete curve has a sharper shape and has sudden failure properties compared to the similar behavior in OPC concrete (Noushini et al., 2016). This indicates that geopolymer concrete has properties that are more brittle than normal concrete containing OPC. Substantially, Wang et al. (2023) revealed that the addition of fiber in the geopolymer concrete mixture can increase compressive strength, flexural strength and toughness.

Structural research on geopolymer concrete carried out by Annamalai et al. (2017) concerned beam structures with an underreinforced reinforcement system made from geopolymer concrete. It was revealed that the flexural strength of beams made of geopolymer concrete was higher than the flexural strength of OPC concrete beams.

Haider et al. (2014) carried out triaxial tests on geopolymer concrete with a compressive strength of 25 MPa and high-strength concrete with a compressive strength of 85 MPa. The test results revealed that to achieve adequate ductility, normal-strength geopolymer concrete requires a tightness level that is not excessively high (confinement ratio < 0.4). However, high-strength geopolymer concrete requires a higher level of confinement, namely around 0.53, to achieve adequate ductility. The results are indications that the ductility properties of geopolymer concrete are like the ductility properties of OPC concrete: the higher the compressive strength of the concrete, the lower the strength and ductility so that a higher level of confinement is required. The consequence of this is that in its application to column structures, it requires confining reinforcement with a volumetric ratio; that is increasingly higher if the compressive strength of the concrete used is higher.

Meanwhile, the behavior of geopolymer concrete against triaxial loads studied by Wang et al. (2020) found that the increase in the strength of confined concrete (K) of geopolymer concrete was not considerably different from the increase in the strength of confined concrete in OPC concrete. In fact, the proposed K -value equation adopts the equation used in OPC concrete because the experimental results indicate similarities with the existing equation.

The behavior of geopolymer concrete towards passive confinement that has been carried out can be found in Lokuge and Karunasena (2016), Alzebaree et al. (2020) and Abadel (2023). The passive confinement used is fiber-reinforced polymer (FRP), which is wrapped around the surface of the geopolymer concrete cylinder. The results of the tests carried out revealed that there was an increase in the strength and ductility of geopolymer concrete confined with the FRP confinement. Meanwhile, Ajmal et al. (2023) revealed that geopolymer concrete confined masonry is higher in initial stiffness and ultimate seismic capacity (around 45% and 4%) compared OPC concrete.

Based on the published data, research on the behavior of geopolymer concrete confined by transverse reinforcement for square cross-sections was carried out by, among others Lokuge et al. (2015), Du et al. (2022), Herwani et al. (2022), and Sudha et al. (2022). The results of the research state that because of confinement by transverse reinforcement installed in square cross-section specimens, the characteristics of transverse reinforcement, like volumetric ratio, spacing, and reinforcement configuration play a significant role in influencing the strength and ductility of confined concrete. Meanwhile, Ganesan et al. (2014) and Muslikh et al. (2018) tested round-section geopolymer concrete cylinders confined by hoops. The test results revealed the ductility of confined geopolymer concrete was lower than the ductility of confined OPC concrete.

Testing of geopolymer concrete confined by transverse reinforcement is still open to further research by reviewing more specific transverse reinforcement design parameters, such as spacing, volumetric ratio, and yield stress. Based on the description above, it raises the hypothesis that the installation of transverse reinforcement in column structures will play a significant role in determining the strength and ductility of geopolymer concrete columns.

Research significance and objective

An investigation of the behavior of confined geopolymer concrete will be extremely useful as a reference to describe the strength and ductility properties of confined geopolymer concrete as a whole. Confinement by transverse reinforcement in geopolymer concrete is absolutely vital because of the brittle nature of geopolymer concrete. The design equations resulting from research on geopolymer concrete confined by transverse reinforcement are extremely useful for more recent application in column structures. A review of existing confined models is absolutely necessary to determine the extent of their accuracy in predicting

experimental results for confined geopolymer concrete. This research aims to explore more thoroughly the stress–strain behavior of geopolymer concrete confined by transverse reinforcement, especially its strength and ductility behavior. The tests carried out are still limited to confined on round cross-sections. Analytical expressions will be derived from the results of this research based on test results.

Experimental program

This research was experimentally carried out by producing a number of specimens and testing them in the laboratory. Twelve geopolymer concrete cylinders were then installed with confining reinforcement in the form of hoops designed by varying the characteristics of the hoop reinforcement, namely spacing, volumetric ratio, and yield stress. Apart from that, three geopolymer concrete cylindrical specimens were also made, which had the same dimensions as the confined concrete specimens, but without confining reinforcement. This specimen is a control for confined concrete specimens.

Materials

The fine aggregate and coarse aggregate used were from the local area. The aggregate test results are as follows: the coarse aggregate has a bulk density of $1,607 \text{ kg}\cdot\text{m}^{-3}$ and a fineness modulus of 6.6. Meanwhile for fine aggregate, the weight of the contents is $1,235 \text{ kg}\cdot\text{m}^{-3}$ and the fineness modulus is 2.68. The fly ash comes from waste from electric steam power plant (PLTU) Tanjung Jati, Central Java, Indonesia. The fly ash used weighs $561.6 \text{ kg}\cdot\text{m}^{-3}$.

The test results analyzed the chemical composition of fly ash using SEM-EDS to determine the shape, size, and elemental composition contained in the fly ash (Fig. 1). The fly ash used is type F. Based on the data in Table 1, CaO content is 5.89% ($< 10\%$), SO_3 content is 1.13% ($< 5\%$), and sum of SiO_2 , Al_2O_3 and Fe_2O_3 equals 83.28% ($> 70\%$). This value complies with the requirements of ASTM C 618-05 standard (American Society for Testing and Materials [ASTM], 2005) for type F fly ash. In this research, the alkali activator solution used was eight-molar sodium hydroxide (NaOH) and a 58% concentration of sodium silicate (Na_2SiO_3) with a ratio of one NaOH to two Na_2SiO_3 .

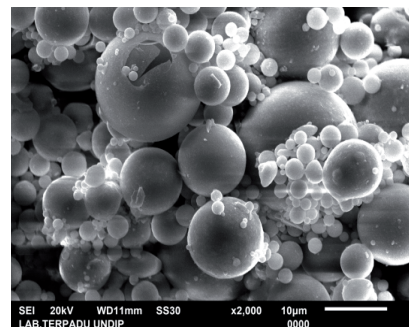


FIGURE 1. Scanning electron microscopy test of coal ash material

Source: own work.

TABLE 1. Chemical composition of Tanjung Jati fly ash (type F)

Composition [%]									
Na ₂ O	MgO	Al ₂ O ₃	SiO ₂	SO ₃	K ₂ O	CaO	Fe ₂ O ₃	TiO ₂	CuO
1.59	2.86	24.95	46.52	1.13	2.77	5.89	11.81	1.36	1.12

Source: own work.

Mix design of geopolymer concrete

The compressive strength of the designed concrete represents normal strength. The composition of the geopolymer concrete mixture is presented in Table 2. The treatment used the ambient temperature. The process of making geopolymer concrete from mixing to curing is shown in Figure 2.

TABLE 2. Mix design

Material	Composition [kg·m ⁻³]
Coarse aggregate	1 209.6
Sand	806.4
Fly ash	561.6
NaOH (eight-molar)	100.8
Natrium silicate	201.6

Source: own work.

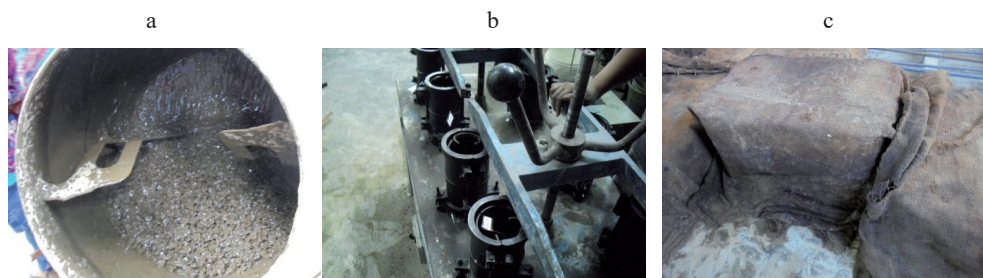


FIGURE 2. Process for making geopolymer concrete: a – mixing process of geopolymer concrete; b – geopolymer concrete mold with transverse reinforcement; c – treatment process using wet sacks

Source: own work.

Specimen of confined concrete

The confining reinforcement is in the form of a plain round hoop with a diameter between 5.5 mm and 6 mm. Each reinforcement is tensile tested to determine the yield stress, strain hardening behavior, and ultimate stress. The tensile test result curve is shown in Figure 3. The design parameters studied are spacing, volumetric ratio, and yield stress of transverse reinforcement.

The specimens are cylindrical, 100 × 200 mm in size. All specimens come without a concrete cover. To maintain the stability of the confining reinforcement, both during

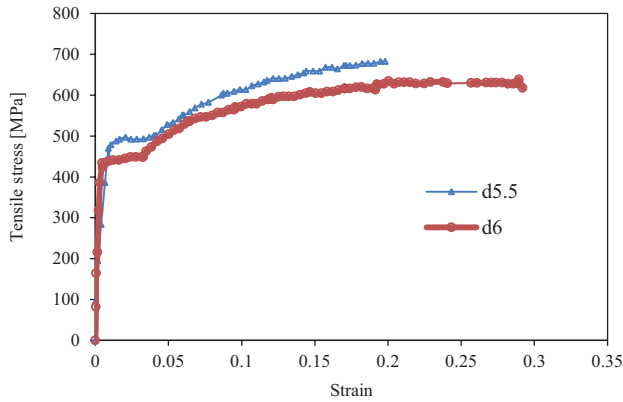


FIGURE 3. Stress–strain curves of hoops

Source: own work.

casting and during testing, four wires were installed in the longitudinal direction as hoop ties. The diameter of the longitudinal wire is extremely small that its influence in the calculation of confined concrete stresses can be neglected. A strain gage of type FLA-6-11 is installed in the confining reinforcement.

Testing and data acquisition

Figure 4 illustrates a test scheme for unconfined and confined geopolymer concrete using the universal testing machine (UTM). It has an effective capacity of 1,800 kN and a displacement control system. On the right and left of the specimen, an LVDT is installed to record the displacement in the axial direction, which is then processed into axial strain data. Cables from the LVDT, load cell and strain gauge are then connected to the Data Logger to record data (including load increments) until the specimen failures. Confined concrete stress is obtained from the load received by the specimen divided by the cross-sectional area of the specimen.

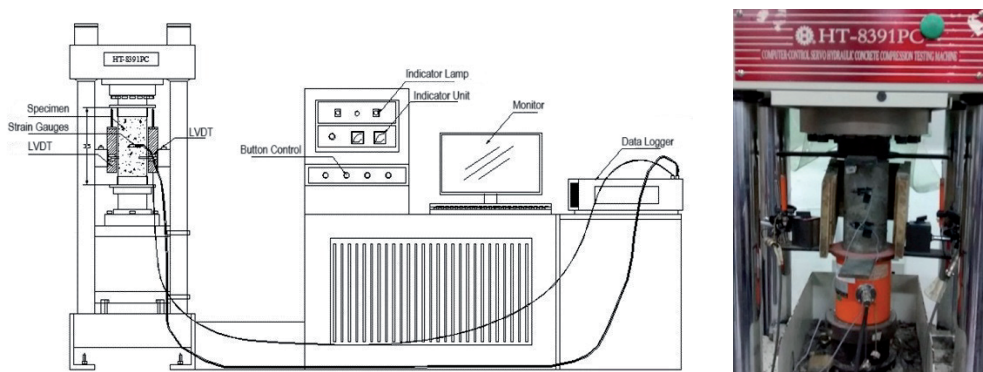


FIGURE 4. Unconfined and confined geopolymer concrete test: a – scheme of testing; b – specimen samples and test preparation

Source: own work.

The test results are then processed into a stress–strain curve. The parameters of the unconfined concrete test results reviewed include peak stress (f_{co}'), peak strain (ϵ_{co}'), and strain when the stress drops 15% of the peak stress (ϵ_{85}). Furthermore, the parameters for confined concrete displayed consist of peak stress (f_{cc}'), peak strain (ϵ_{cc}'), and strain when the stress drops 15% of the peak stress (ϵ_{85c}). The ductility of confined concrete (μ) is defined as the ratio of the value ϵ_{85c} to the value ϵ_{85c} (see Fig. 5).

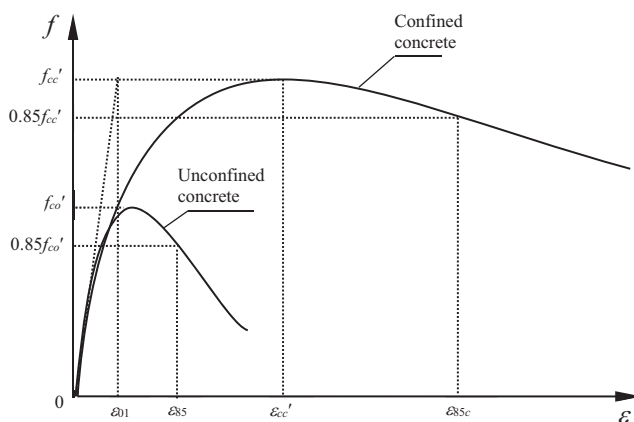


FIGURE 5. Parameter design of unconfined and confined geopolymer concrete

Source: own work.

Results and discussion

In this experiment, all specimens were tested on the same day (including unconfined concrete). So that the comparison results between the confined (CGP) and unconfined geopolymer concrete (UGP) test results could be measured with certainty. From the material testing results, the average Poisson's ratio value for geopolymer concrete was obtained at 0.25, and the average modulus of elasticity was 26.986 MPa. The results for the unconfined concrete obtained the average value of three specimens, namely $\epsilon_{co}' = 0.0026$, $\epsilon_{85} = 0.0034$ and $f_{co}' = 36.28$ MPa. The ϵ_{co}' value is above the value usually assumed for normal concrete (0.002–0.0022). Figure 6 shows the failure modes of unconfined geopolymer concrete (UGP) specimens. Similar to the results of other research on the behavior of geopolymer concrete, the results of this research also indicate the process of failure of unconfined and brittle geopolymer concrete.

Confined geopolymer concrete specimens installed with hoops with tighter spacing ($s = 60$ mm) showed a relatively ductile failure mode (Fig. 7a). Lateral expansion due to

uniaxial compressive loads can be inhibited or controlled by hoop reinforcement so that the concrete core is completely undamaged. For the present, specimens installed with hoops with wider spacing ($s = 100$) had a faster failure mode (Fig. 7b).

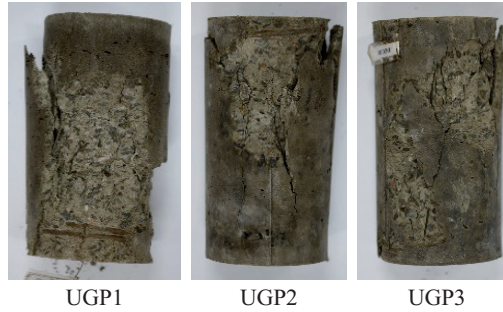


FIGURE 6. Failure pattern of unconfined geopolymer concrete (UGP)

Source: own work.

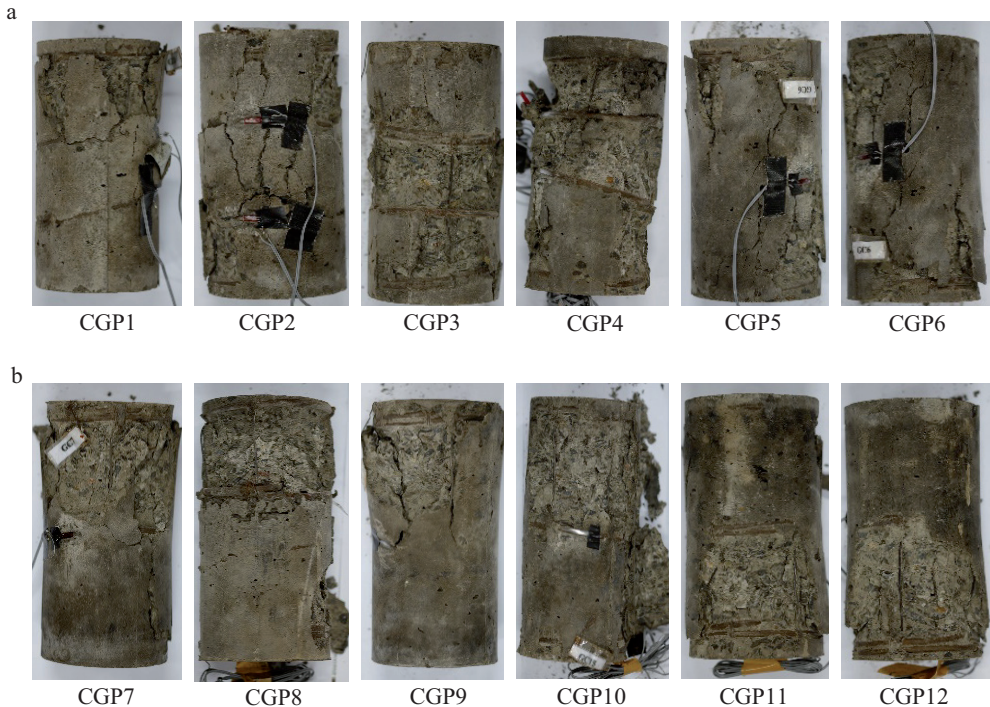


FIGURE 7. Failure pattern of confined geopolymer concrete: a – CGP specimen, hoop spacing 60 mm; b – CGP specimen, hoop spacing 100 mm

Source: own work.

As explained in the experimental program above in Table 3, there are four confined groups, each consisting of three specimens with the same confining reinforcement installation characteristics like: diameter, spacing, and yield stress. Table 3 explained in Figure 8, shows that the K value will be optimal if the confining reinforcement has an increased volumetric ratio, but the yield stress is lower ($f_y = 466$ MPa). This can be seen from the comparison between CGP1, CGP2, and CGP3 (average K of 1.44) specimens and CGP4, CGP5, and CGP6 specimens, which have a higher average K value of 1.53. The K value is also optimal in comparison between CGP7, CGP8, and CGP9 specimens (average $K = 1.22$) and specimens CGP10, CGP11 and CGP12 (average $K = 1.26$).

TABLE 3. Experimental results

Specimen	Confining reinforcement			f_{cc}' [MPa]	ε_{cc}'	ε_{85c}	$K = \frac{f_{cc}'}{f_{co}'}$	K_{avg}	μ	μ_{avg}
	$\phi-s$ [mm]	ρ_h	f_y [MPa]							
CGP1	5.5–60	0.0168	514	52.30	0.0095	0.0321	1.44	1.44	17.89	17.65
CGP2	5.5–60	0.0168	514	52.30	0.0069	0.0240	1.44		20.00	
CGP3	5.5–60	0.0168	514	52.78	0.0084	0.0286	1.45		15.05	
CGP4	6–60	0.0200	466	55.42	0.0075	0.0266	1.53	1.53	13.64	14.50
CGP5	6–60	0.0200	466	55.43	0.0058	0.0311	1.53		17.28	
CGP6	6–60	0.0200	466	56.03	0.0066	0.0176	1.54		12.57	
CGP7	5.5–100	0.0101	514	40.17	0.0039	0.0091	1.24	1.22	5.93	5.94
CGP8	5.5–100	0.0101	514	38.89	0.0035	0.0080	1.22		6.58	
CGP9	5.5–100	0.0101	514	40.33	0.0043	0.0097	1.21		5.31	
CGP10	6–100	0.0120	466	38.82	0.0049	0.0080	1.27	1.26	5.93	5.76
CGP11	6–100	0.0120	466	40.46	0.0043	0.0080	1.22		5.71	
CGP12	6–100	0.0120	466	41.06	0.0047	0.0079	1.29		5.64	

Source: own work.

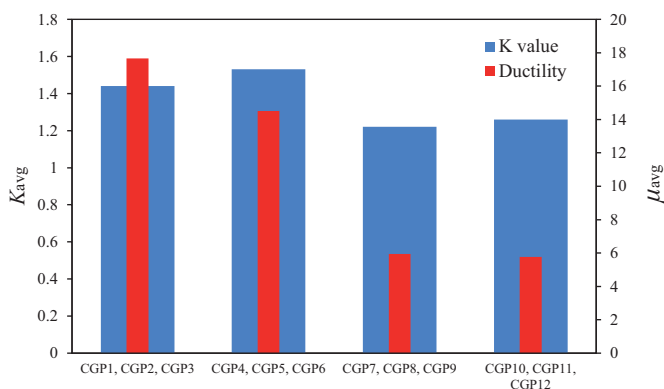


FIGURE 8. Comparison of average K and ductility (μ_{avg}) values

Source: own work.

However, the opposite occurs in the magnitude of the ductility value of confined concrete where the optimum μ value occurs if the specimen is installed with confining reinforcement with a lower volumetric ratio but the yield stress is higher. The average ductility value of CGP1, CGP2, and CGP3 specimens is 17.65, which is higher than the average ductility of CGP4, CGP5, and CGP6 specimens ($\mu = 14.50$). Likewise, the average ductility of CGP7, CGP8, and CGP9 specimens is 5.94, which is still higher than the average ductility of CGP10, CGP11, and CGP12 specimens of 5.76.

Another phenomenon is that even though the spacing of the confining reinforcement installed is the same as the diameter of the specimen (CGP7, CGP8, CGP9, CGP10, CGP11, CGP12). There is still an increase in the strength of the confined concrete, although it is not significant ($K > 1.2$). Similarly, the ductility of confined concrete is still above 5. This phenomenon is not the same as what occurs in confined OPC concrete which states that there is no increase in the K value (or the same as in unconfined concrete); if the spacing of the confining reinforcement is the same as the cross-sectional diameter (Antonius et al., 2017).

Stress–strain behavior

Figures 9 and 10 show that in general, three specimens in one group that have the same confining reinforcement characteristics (for example, CGP1, CGP2, CGP3, and other specimen groups) have stress–strain curve shapes that almost coincide with each other.

As mentioned above, the ε_{co}' value which is greater than the ε_{co} value usually assumed for normal concrete (OPC concrete). However, the post-peak behavior of unconfined concrete (UGP) is very brittle; where after the peak there is an extremely rapid decline in the

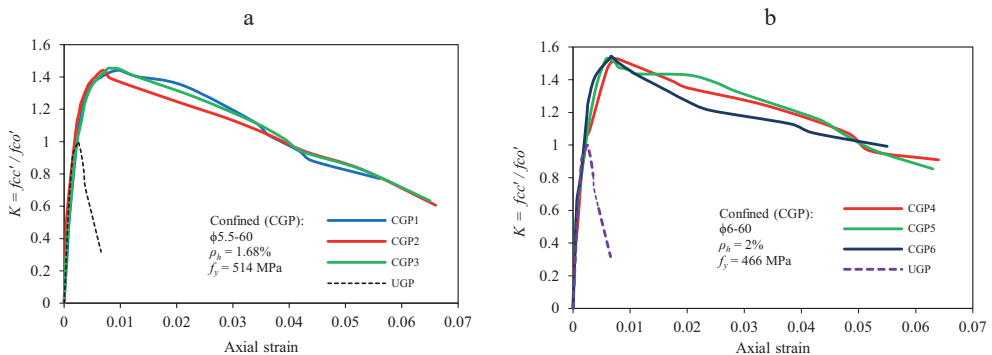


FIGURE 9. Behavior of confined versus unconfined geopolymer concrete (hoop spacing 60 mm): a – specimen CGP1, CGP2 and CGP3 versus UGP; b – specimen CGP4, CGP5 and CGP6 versus UGP

Source: own work.

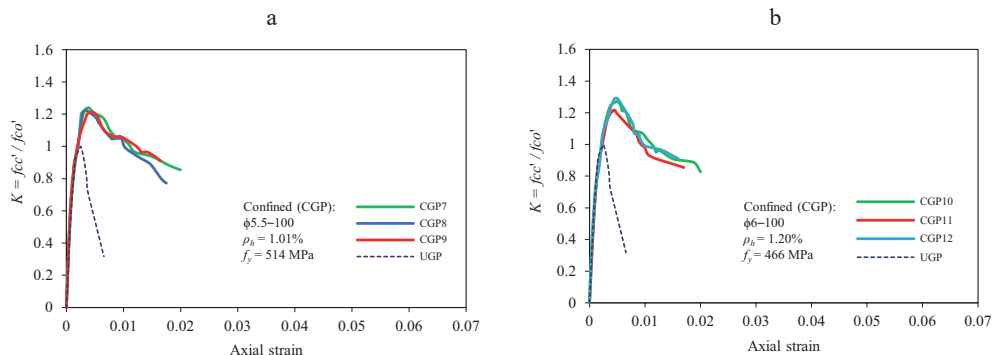


FIGURE 10. Behavior of confined versus unconfined geopolymer concrete (hoop spacing 100 mm): a – specimen CGP7, CGP7, CGP9 versus UGP; b – specimen CGP10, CGP11 and CGP12 versus UGP
Source: own work.

curve. This is in line with the results of several studies on the mechanical properties of geopolymer concrete, which state that geopolymer concrete is very brittle (Noushini et al., 2016; Muslikh et al., 2018). Therefore, installing confining reinforcement is a necessity to improve the extremely low ductility of geopolymer concrete.

In line with the results shown in Table 3, installing tighter hoop spacing has an extremely beneficial confining effect and can increase the K value and ductility of confined geopolymer concrete. As shown in Figure 11, the post-peak curve is relatively flat. The phenomenon of changes in K values and ductility due to the influence of transverse reinforcement spacing; is the same as the results of confined geopolymer concrete tests carried out by Herwani et al. (2022), but the specimen used represent a square cross-section.

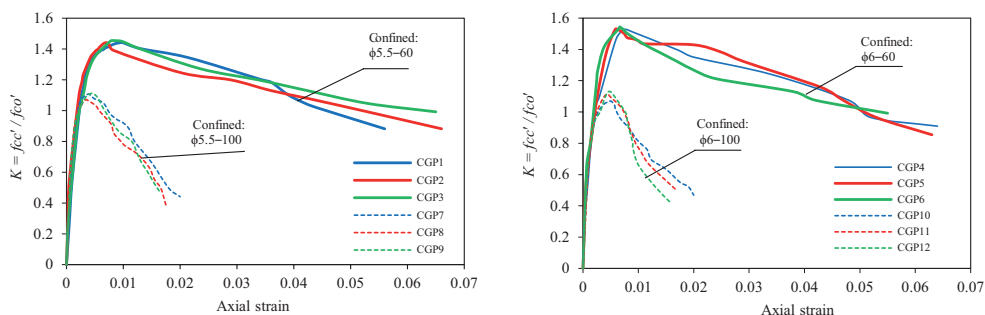


FIGURE 11. Effect of confining reinforcement spacing
Source: own work.

Evaluation of confinement models

Confinement models are necessary to determine and ensure the level of structural safety. Until now, geopolymer concrete confinement models were based on passive confinement test results, namely concrete confined by transverse reinforcement. The recorded publication states that the confinement models derived from the results of passive confined testing are the model proposed by Ganesan et al. (2014) for round-section specimens, and the model proposed by Lokuge et al. (2015) for square-section columns. Confinement models resulting from triaxial tests, where the level of confinement can be regulated and its size determined with certainty include the model proposed by Haider et al. (2014) and the model by Wang et al. (2020). Further, we will evaluate both Mander's proposed confinement model and Ganesan's proposed model as well as Wang's proposed model to consider these models are applicable to the cross-section used in this research.

Model by Mander et al. (1988)

Mander's confinement model is widely known and is often used as a reference for confined concrete research. The model is basically derived from the test results of normal concrete (OPC concrete) columns. Mander's model can be applied to confined concrete of round cross-section and square cross-section. Mander et al. (1988) uses one equation to describe the stress–strain curve of confined concrete, namely:

$$f_c = \frac{f_{cc}' \frac{\varepsilon_c}{\varepsilon_{cc}'}}{r - 1 + \left(\frac{\varepsilon_c}{\varepsilon_{cc}'} \right)^r}, \quad (1)$$

where:

$$\frac{\varepsilon_{cc}'}{\varepsilon_{co}'} = 1 + 5 \left(\frac{f_{cc}'}{f_{co}'} - 1 \right), \quad (2)$$

$$r = \frac{E_c}{E_c - E_{sec}}, \quad (3)$$

$$E_c = 5,000 \sqrt{f_{co}'} \text{ MPa}. \quad (4)$$

E_{sec} is the secant modulus, i.e.:

$$E_{\text{sec}} = \frac{f'_{cc}}{\epsilon'_{cc}}. \quad (5)$$

Mander uses the Willam–Warnke failure criterion (five parameters) to derive the peak-stress equation for confined concrete. The proposed equation is:

$$K = \frac{f'_{cc}}{f'_{co}} = -1.254 + 2.254 \sqrt{1 + \frac{7.94 f'_l}{f'_{co}}} - 2 \frac{f'_l}{f'_{co}}, \quad (6)$$

where f'_l is the effective lateral stress.

Model by Ganesan et al. (2014)

The geopolymer concrete confinement model proposed by Ganesan et al. (2014) basically uses most of the equations from Mander mentioned in previous section, where the stress–strain equation uses Eq. (1). However, Ganesan carried out the necessary modifications after testing 24 specimens of confined geopolymer concrete cylinders and normal confined concrete. The modifications made by Ganesan were to the values:

$$r = \frac{E_c}{\frac{E_c}{1.62} + 8,888k}, \quad (7)$$

and

$$E_c = 6,965 \sqrt{f_{ck}}, \quad (8)$$

where f_{ck} is the compressive strength of the concrete, and k is the confinement index namely:

$$k = \frac{\rho f_y}{f'_c}. \quad (9)$$

Lateral stress is calculated as follows:

$$f_l = \frac{\rho f_y}{2}. \quad (10)$$

Based on Eq. (10), Ganesan assumes that the confining reinforcement yields when the concrete peak response is confined.

Model by Wang et al. (2020)

Wang et al. (2020) carried out triaxial tests on a number of cylindrical geopolymer concrete specimens that possessed compressive strengths of 15 MPa and 85 MPa. Lateral stress is provided by fluid pressure, with pressures ranging from 0 MPa to 35 MPa. Wang proposed the peak stress of confined concrete (f_{cc}) as follows:

$$f_{cc} = f_c + 5.2 f_c^{0.91} \left(\frac{\sigma_l}{f_c} \right)^{\alpha}, \quad (11)$$

where f_c is the unconfined compressive strength of concrete, and α :

$$\alpha = f_c^{-0.006}. \quad (12)$$

The peak strain of confined concrete (ε_{cc}) is derived from the results of non-linear regression using data from experiments carried out and produces:

$$\varepsilon_{cc} = \varepsilon_0 \left[1 + 13.446 \left(\frac{\sigma_l}{f_c} \right)^{1.2299} \right], \quad (13)$$

where σ_l is the lateral stress and ε_0 is the unconfined peak strain of concrete which is taken as 0.00225. The confined geopolymer concrete stress–strain curve refers to Mander's equation, namely Eq. (1), but the r equation is modified to:

$$r = \frac{k_r E_c}{E_c - E_{sec}} = \frac{k_r E_c}{E_c \frac{f_{cc}}{\varepsilon_{cc}}}. \quad (14)$$

The k_r value is:

$$k_r = \sqrt{\frac{f_c}{30}}. \quad (15)$$

Comparison of confinement models with experimental results

The above-mentioned confinement models were further validated with experimental results from this research. As seen in Figures 12 and 13, the confinement model by Mander, Ganesan, and Wang has a non-linear and concave post-peak curve. This behavior is differ-

ent from the experimental results of this research, where the post-peak behavior tends to be convex. The difference in the curve's shape is because the confined models assume that confined geopolymer concrete loses post-peak strength more quickly; compared to the post-peak strength loss from the test results.

In general, the peak stress of confined concrete (f_{cc}') based on confined models is not considerably different from the f_{cc}' value from experimental results. However, the existing confinement models underestimate the post-peak behavior of the experimental results if the confinement reinforcement spacing is 60 mm (Fig. 10). Furthermore, Figure 11 explains that except for Wang's proposed model, other confinement models are absolutely accurate in predicting: the f_{cc}' value from experimental results if the specimen is installed with confining reinforcement with larger spacing ($s = 100$ mm). However, the post-peak behavior of all confinement models overestimates the post-peak behavior of the experimental results.

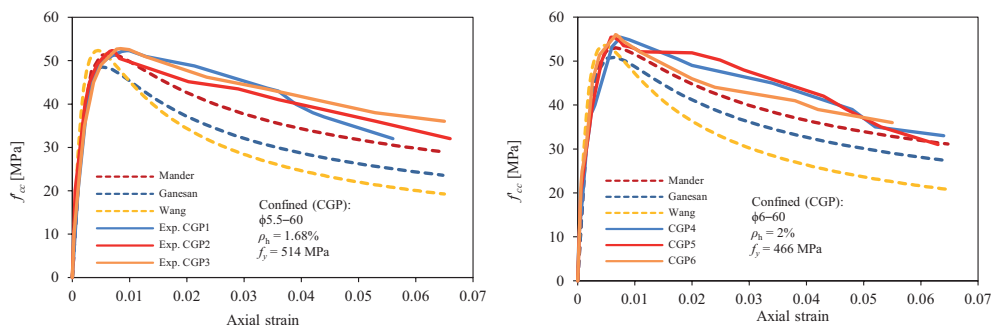


FIGURE 12. Confinement models vs experimental specimens with hoop spacing of 60 mm

Source: own work.

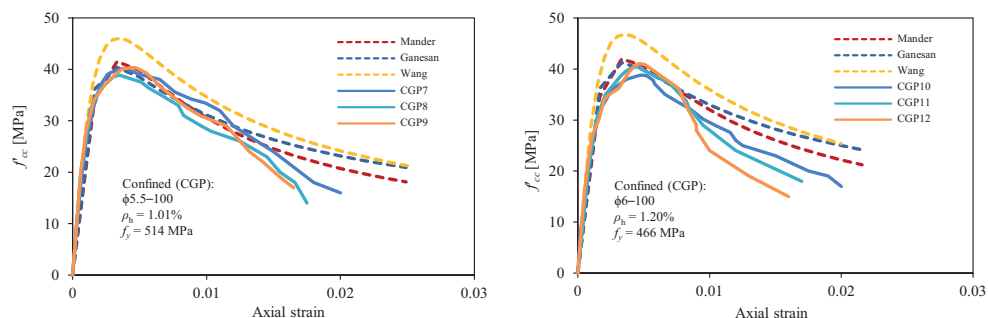


FIGURE 13. Confinement models vs experimental specimens with hoop spacing of 100 mm

Source: own work.

Analytical expression of confined geopolymer concrete

The results of the comparison between the confined models and the experimental results above show that the peak stress value of confined concrete is not considerably different from the experimental results: except for Wang's proposed model if wider stirrups are installed on the specimen (in this case, the hoop spacing is the same as the core diameter of the concrete cross section.). In addition, predictions of post-peak behavior also differ from experimental results. Based on this fact, there was an attempt to develop an analytical expression of the stress–strain behavior of confined geopolymer concrete from the experimental results above. Analytical expression is carried out by modifying the existing confinement model as necessary. Strength enhancement of confined geopolymer concrete (K) has a very significant role in determining the volumetric ratio of the minimum confining reinforcement that must be installed in the column structure. The K -value equation uses the equation proposed by Haider et al., which was derived based on the test results of geopolymer concrete with active confined, namely:

$$K = \frac{f'_{cc}}{f'_{co}} = 1 + 3.3 \left(\frac{f_2}{f'_{co}} \right)^{0.8}, \quad (16)$$

where f_2 represents the lateral stress. The f_2 value uses Eq. (10). The lateral stress is corrected by the effectiveness of the confinement, which uses the proposal of Mander et al., that is:

$$k_e = \frac{\left(1 - \frac{s'}{2d_c} \right)}{(1 - \rho_{cc})}. \quad (17)$$

In Eq. (17), s' is the clear spacing of confining reinforcement, d_c is the core diameter of the concrete section, and ρ_{cc} represents the ratio of longitudinal reinforcement to the core area of the section. The peak strain of confined concrete compared to the peak strain of unconfined concrete represents a function of the K value, and the results of non-linear regression from experimental data produce the equation (Fig. 14):

$$\frac{\epsilon'_{cc}}{\epsilon'_{co}} = 1 + 4.9845(K - 1)^{1.3716}. \quad (18)$$

The unconfined concrete peak strain (ϵ'_{co}) is assumed to be 0.002.

The confined concrete stress–strain curve is divided into two parts, namely the ascending branch curve, which uses Eq. (1). The r and k values use the formulation by Ganesan values, namely Eqs (7) and (9). The modulus of elasticity uses the equation proposed by Romadhon et al. (2022), which is:

$$E_c = 2,673 f_c^{0.65} \tag{19}$$

Furthermore, the post-peak confined geopolymer concrete curve, or the one that represents the ductility behavior of the structure is assumed to be linear. The curve equation is:

$$f_c = f_{cc}' - (\varepsilon_c - \varepsilon_{cc}') \frac{0.15 f_{cc}'}{(\varepsilon_{85c} - \varepsilon_{cc}')} \tag{20}$$

Similar to the derivation of the peak-strain equation for confined concrete above, the ductility of confined concrete is also derived based on experimental data using non-linear regression as follows (Fig. 15):

$$\frac{\varepsilon_{85c}}{\varepsilon_{85}} = 1 + 23.71(K - 1)^{1.9226} \tag{21}$$

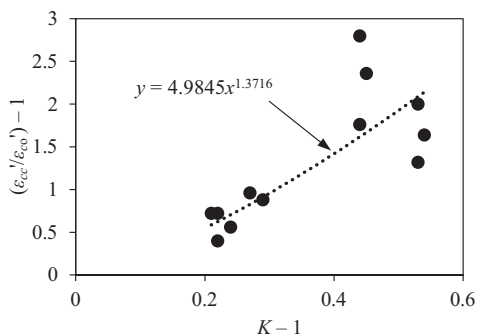


FIGURE 14. Regression of ε_{cc}' values
Source: own work.

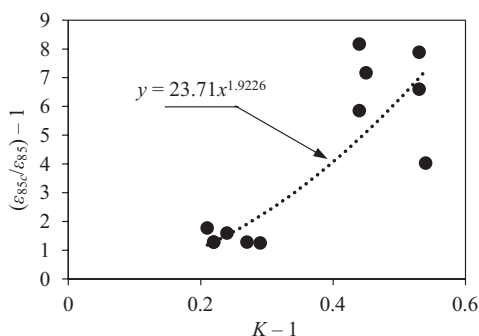


FIGURE 15. Regression of ε_{85c} values
Source: own work.

Comparison of analytical expressions with experimental results

Figures 16 and 17 are a comparison of the stress–stress behavior of confined geopolymer concrete with experimental results. Based on these Figures, the developed analytical expressions are able to predict the stress behavior of the pre-peak confined geopolymer concrete very well. Furthermore, the analytical expression on the post-peak curve has a line shape that is in line with and very close to the post-peak behavior of the experimental results.

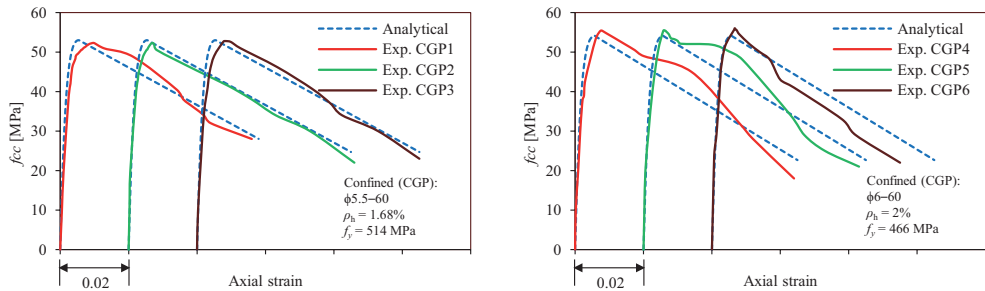


FIGURE 16. Analytical expression versus experimental results for specimens with confining reinforcement spacing of 60 mm

Source: own work.

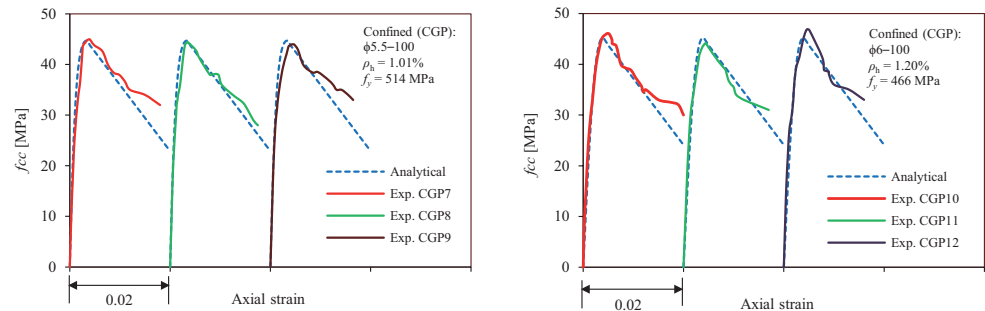


FIGURE 17. Analytical expression versus experimental results for specimens with confining reinforcement spacing of 100 mm

Source: own work.

Conclusions

The investigation of the behavior of confined geopolymer concrete has been carried out by conducting experimental tests. Some of the conclusions obtained are as follows:

1. Geopolymer concrete has a very brittle behavior, which can be seen in the behavior of unconfined geopolymer concrete. However, by installing confining reinforcement with a relatively high volumetric ratio and tighter spacing, the behavior of geopolymer concrete changes to become very ductile.
2. In general, the strength of confined geopolymer concrete increases along with the installation of tighter confining reinforcement. This increase in strength is also in line with the increase in ductility of confined concrete.
3. Based on experimental results, the K value will be optimal if geopolymer concrete is installed with confining reinforcement with an increased volumetric ratio but decreased yield stress. However, on the contrary, the optimum ductility value will occur if the confining reinforcement has a volumetric ratio that tends to be lower but the yield stress increases.
4. Even though the spacing of the confining reinforcement installed is the same as the cross-sectional diameter of the concrete core, the confined geopolymer concrete still has a fairly good K value (average K value above 1.2).
5. Except for Wang's proposed model, the existing confinement models made of OPC concrete and geopolymer concrete are generally not completely different in predicting the peak stress value from experimental results.
6. The ductility behavior of confined concrete based on existing confined models is still significantly different from the ductility behavior of experimental results.
7. The analytical expression for confined geopolymer concrete, which was developed based on modification of the existing confined model and the derivation of several equations from experimental data, is able to predict: the K value, pre-peak and post-peak behavior very well.

Acknowledgments

The experimental work in this research performed in laboratory of structures, Diponegoro University. The support received for this research is gratefully acknowledged.

References

- Abadel, A. A. (2023). Structural performance of strengthening of high-performance geopolymer concrete columns utilizing different confinement materials: experimental and numerical study. *Buildings*, 13 (7), 1709. <https://doi.org/10.3390/buildings13071709>
- Ajmal, M. M., Qazi, A. U., Ahmed, A., Mughal, U. A., Abbas, S., Kazmi, S. M. S., & Munir, M. J. (2023). Structural performance of energy efficient geopolymer concrete confined masonry: an approach towards decarbonization. *Energies*, 16 (8), 3579. <https://doi.org/10.3390/en16083579>

- Alzebaree, R., Çevik, A., Mohammedameen, A., Niş, A., & Gülşan, M. E. (2020). Mechanical performance of FRP-confined geopolymer concrete under seawater attack. *Advances in Structural Engineering*, 23 (6), 1055–1073. <https://doi.org/10.1177/1369433219886964>
- American Concrete Institution [ACI]. (2002). *The use of fly ash in concrete* (ACI 232 2R-96). American Concrete Institution. http://civilwares.free.fr/ACI/MCP04/2322r_96.pdf
- American Society for Testing and Materials [ASTM]. (2005). *Standard specification for coal fly ash and raw or calcined natural pozzolan for use* (ASTM C 618-05). American Society for Testing and Materials.
- Annamalai, S., Thirugnanasambandam, S., & Muthumani, K. (2017). Flexural behaviour of geopolymer concrete beams cured under ambient temperature. *Asian Journal of Civil Engineering*, 18 (4), 621–631.
- Antonius, Imran, I., & Setiawan, P. (2017). On the confined high-strength concrete and need of future research. *Procedia Engineering*, 171, 121–130. <https://doi.org/10.1016/j.proeng.2017.01.318>
- Bouzoubaâ, N., Zhang, M. H., & Malhotra, V. M. (1999). Production and performance of laboratory produced high volume fly ash blended cements in concrete. In *ACI international symposium on concrete technology for sustainable development* (pp. 1-13). International Centre for Sustainable Development of Cement and Concrete (ICON).
- Diaz-Loya, E. I., Allouche, E. N., & Vaidya, S. (2011). Mechanical properties of fly-ash-based geopolymer concrete. *ACI Materials Journal*, 108 (3), 300–306. <https://doi.org/10.14359/51682495>
- Du, D. F., Wang, J. H., Wang, X., & Su, C. (2022). Compressive behavior and stress-strain model of square confined ambient-cured fly ash and slag-based geopolymer concrete. *Case Studies in Construction Materials*, 17 (June). <https://doi.org/10.1016/j.cscm.2022.e01203>
- Ekaputri, J. J., & Triwulan. (2011). Geopolymer concrete using fly ash, trass, Sidoarjo Mud based material. *Journal of Civil Engineering*, 31 (2), 57–63. <http://dx.doi.org/10.12962/j20861206.v31i2.1466>
- Ganesan, N., Abraham, R., Raj, S. D., & Sasi, D. (2014). Stress-strain behaviour of confined Geopolymer concrete. *Construction and Building Materials*, 73, 326–331. <https://doi.org/10.1016/j.conbuildmat.2014.09.092>
- Haider, G. M., Sanjayan, J. G., & Ranjith, P. G. (2014). Complete triaxial stress-strain curves for geopolymer. *Construction and Building Materials*, 69, 196–202. <https://doi.org/10.1016/j.conbuildmat.2014.07.058>
- Hardjito, D., Wallah, S. E., Sumajouw, D. M. J., & Rangan, B. V. (2004). On the development of fly ash-based geopolymer concrete. *ACI Materials Journal*, 101 (6), 467–472. <https://doi.org/10.14359/13485>
- Herwani, H., Imran, I., Budiono, B., & Zulkifli, E. (2022). Strength enhancement, ductility, and confinement effectiveness index of fly ash-based geopolymer concrete square columns. *Journal of Engineering and Technological Sciences*, 54 (4), 1–16. <https://doi.org/10.5614/j.eng.technol.sci.2022.54.4.11>
- Lokuge, W., & Karunasena, W. (2016). Ductility enhancement of geopolymer concrete columns using fibre-reinforced polymer confinement. *Journal of Composite Materials*, 50 (14), 1887–1896. <https://doi.org/10.1177/0021998315597553>

- Lokuge, W., Sanjayan, J., & Setunge, S. (2015). Use of geopolymer concrete in column applications. In *Proceedings of the 27th Biennial National Conference of the Concrete Institute of Australia* (pp. 1-8). University of Southern Queensland. <https://research.usq.edu.au/item/q3523/use-of-geopolymer-concrete-in-column-applications>
- Mander, J. B., Priestley, M. J., & Park, R. (1988). Theoretical stress-strain model for confined concrete. *Journal of Structural Engineering*, 114 (8), 1804–1826. [https://doi.org/10.1061/\(ASCE\)0733-9445\(1988\)114:8\(1804\)](https://doi.org/10.1061/(ASCE)0733-9445(1988)114:8(1804))
- Muslikh, Anggraini, N. K., Hardjito, D. & Antonius (2018). Behavior of geopolymer concrete confined with circular hoops. *MATEC Web of Conferences*, 159, 1–7. <https://doi.org/10.1051/matec-conf/201815901018>
- Nagajothi, S., Elavenil, S., Angalaeswari, S., Natrayan, L., & Mammo, W. D. (2022). Durability studies on fly ash based geopolymer concrete incorporated with slag and alkali solutions. *Advances in Civil Engineering*, 2022, 7196446. <https://doi.org/10.1155/2022/7196446>
- Noushini, A., Aslani, F., Castel, A., Gilbert, R. I., Uy, B., & Foster, S. (2016). Compressive stress-strain model for low-calcium fly ash-based geopolymer and heat-cured Portland cement concrete. *Cement and Concrete Composites*, 73, 136–146. <https://doi.org/10.1016/j.cemconcomp.2016.07.004>
- Owaid, H. M., Al-Rubaye, M. M., & Al-Baghdadi, H. M. (2021). Use of waste paper ash or wood ash as substitution to fly ash in production of geopolymer concrete. *Scientific Review Engineering and Environmental Sciences*, 30 (3), 464–476. <https://doi.org/10.22630/PNIKS.2021.30.3.39>
- Romadhon, E. S., Antonius, & Sumirin. (2022). Mechanical Properties of Geopolymer Concrete Containing Low-Alkaline Activator. *Annales de Chimie: Science Des Materiaux*, 46 (5), 273–279. <https://doi.org/10.18280/acsm.460506>
- Sudha, C., Sambasivan, A. K., Kannan Rajkumar, P. R., & Jegan, M. (2022). Investigation on the performance of reinforced concrete columns jacketed by conventional concrete and geopolymer concrete. *Engineering Science and Technology, an International Journal*, 36, 101275. <https://doi.org/10.1016/j.jestch.2022.101275>
- Triwulan, M., Ekaputri, J. J., & Priyanka, N. F. (2017). The Effect of Temperature Curing on Geopolymer Concrete. *MATEC Web of Conferences*, 97, 01005. <https://doi.org/10.1051/matec-conf/20179701005>
- Wang, T., Fan, X., Gao, C., Qu, C., Liu, J., & Yu, G. (2023). The influence of fiber on the mechanical properties of geopolymer concrete: A review. *Polymers*, 15 (4), 827. <https://doi.org/10.3390/polym15040827>
- Wang, H., Wu, Y., Wei, M., Wang, L., & Cheng, B. (2020). Hysteretic behavior of geopolymer concrete with active confinement subjected to monotonic and cyclic axial compression: An experimental study. *Materials*, 13 (18), 3997. <https://doi.org/10.3390/ma13183997>
- Wong, L. S. (2022). Durability performance of geopolymer concrete: A review. *Polymers*, 14 (5), 868. <https://doi.org/10.3390/polym14050868>

Summary

Investigation on strength and ductility of confined geopolymer concrete subjected to axial loads. This paper presents the results of an investigation into geopolymer concrete confined by hoop reinforcement. The investigation focused on the strength and ductility of confined geopolymer concrete subjected to axial loads. The main objective of this research is to evaluate the strength and ductility behavior of confined concrete: by varying several confining reinforcement design parameters, like volumetric ratio, spacing, and yield stress. A total of 15 unconfined and confined geopolymer concrete specimens was produced and tested against axial loads. The test is carried out until the specimen collapses. Experimental results show that unconfined geopolymer concrete is highly brittle, characterized by very sharp post-peak behavior. The volumetric ratio, spacing, and yield stress of reinforcement play a significant role in determining the strength and ductility of confined geopolymer concrete. The comparison between the existing restraint models reviewed in the research was able to predict behavior before the peak of the experimental results very well. However, the existing confinement model has significantly different ductility behavior from the ductility behavior of the experimental results. In this research, an analytical expression of stress–strain for confined geopolymer concrete is developed by modifying the existing confinement model. The validation of confined concrete stress–strain between analytical expressions and experimental results is relatively close.